

Hamartin, the tuberous sclerosis complex 1 gene product, interacts with polo-like kinase 1 in a phosphorylation-dependent manner

Aristotelis Astrinidis[†], William Senapedis[†] and Elizabeth P. Henske^{*}

Fox Chase Cancer Center, Philadelphia, PA 19111, USA

Received September 28, 2005; Revised and Accepted November 30, 2005

Tuberous sclerosis complex (TSC) is a tumor suppressor gene syndrome caused by mutations in *TSC1* and *TSC2*. Hamartin and tuberin, the products of *TSC1* and *TSC2*, respectively, form heterodimers and inhibit the mammalian target of rapamycin. Previously, we have shown that hamartin is phosphorylated by CDC2/cyclin B1 during the G₂/M phase of the cell cycle. Here, we report that hamartin is localized to the centrosome and that phosphorylated hamartin and phosphorylated tuberin co-immunoprecipitate with the mitotic kinase Plk1. Plk1 interacts with the N-terminus of hamartin (amino acids 1–880), which contains two potential Plk1-binding sites (T310 and S332). Phosphorylated hamartin interacts with Plk1 independent of tuberin with all three proteins present in a complex. A non-phosphorylatable hamartin mutant with an alanine substitution at residue T310 does not interact with Plk1, whereas a non-phosphorylatable hamartin mutant at residue S332 in conjunction with alanine mutations at the other CDC2/cyclin B1 sites (T417, S584 and T1047) does not impact hamartin binding to Plk1. Hamartin negatively regulates the protein levels of Plk1. Finally, *Tsc1*^{-/-} mouse embryonic fibroblasts (MEFs) have increased number of centrosomes and increased DNA content, compared to *Tsc1*^{+/+} cells. Both phenotypes are rescued after pre-treatment with the mTOR inhibitor rapamycin. RNAi inhibition of Plk1 in *Tsc1*^{-/-} MEFs failed to rescue the increased centrosome number phenotype. These data reveal a novel subcellular localization for hamartin and a novel interaction partner for the hamartin/tuberin complex and implicate hamartin and mTOR in the regulation of centrosome duplication.

INTRODUCTION

Tuberous sclerosis complex (TSC) is a tumor suppressor gene syndrome characterized by benign tumors in the brain, kidney, heart and skin, and neurological features including seizures, mental retardation and autism (1). TSC is caused by inactivating mutations in the *TSC1* and *TSC2* tumor suppressor genes (2,3). The protein products of *TSC1* and *TSC2*, hamartin and tuberin, respectively, form heterodimers (4–6) that inhibit the mammalian target of rapamycin (mTOR). This is achieved via tuberin, which acts as a GTPase-activating protein toward the small GTPase Rheb (7,8). Both hamartin and tuberin have also been implicated in regulation of the cell cycle (9–11), probably mediated in part by the interaction of tuberin with the cyclin-dependent

kinase inhibitor p27 (12,13). Mutations in either *TSC1* or *TSC2* lead to the same human disease, indicating that hamartin is essential for tuberin function; however, hamartin's precise role in the hamartin/tuberin complex is not completely understood.

We recently found that hamartin is phosphorylated by CDC2/cyclin B1 during the G₂/M phase of the cell cycle (14). Mitotic kinases like CDC2/cyclin B1 often prime substrates for interaction with the mitotically active polo-like kinase 1 (Plk1) (15). Plk1 localizes to the centrosome during prophase and metaphase, moves to the mitotic spindle during anaphase and, finally, to the equatorial plate in cytokinesis (16,17). Increases in the level and activity of Plk1 coincide with the onset of mitosis (16). Polo-like kinases are key regulators of cell cycle progression, with

*To whom correspondence should be addressed at: Fox Chase Cancer Center, 333 Cottman Avenue, Philadelphia, PA 19111, USA. Tel: +1 2157282428; Fax: +1 2152141623; Email: elizabeth.henske@fccc.edu

[†]The authors wish it to be known that, in their opinion, the first two authors should be regarded as joint First Authors.

roles in the G₂ to M transition, centrosome maturation, spindle assembly and cytokinesis (reviewed in 18). A hallmark feature of Plks is the highly conserved C-terminal duplicated polo-box domain (PBD). The PBD mediates binding of Plk1 to phosphorylated substrates during mitosis and is required for centrosomal localization of Plk1 yet the protein(s) that target Plk1 to the centrosome are not known (15,19).

The core consensus motif recognized by the Plk1 PBD is S-pT/pS-P-X (15). Hamartin contains three potential Plk1-binding motifs that involve phosphorylation at residues T310, S332 and T1047. Of these, residue T310 is within the most stringent motif for PBD binding (20).

Hamartin's mitotic phosphorylation by CDC2/cyclin B1 and the presence of three potential Plk1-binding motifs led us to ask whether hamartin interacts with Plk1. Here, we report that hamartin localizes to the centrosome, which is the first specific subcellular localization reported for hamartin. A phosphorylated form of hamartin interacts with Plk1 and is dependent on hamartin residue T310, which lies within a Plk1 PBD-binding motif. The interaction of the hamartin/tuberin complex with Plk1 is hamartin-dependent, with all three proteins present in the complex. Hamartin depletion, either by RNA interference (RNAi) or in *Tsc1*^{-/-} mouse embryonic fibroblasts (MEFs), increases Plk1 protein levels. *Tsc1*^{-/-} MEFs have increased number of centrosomes, compared to their hamartin-proficient counterparts, suggesting that hamartin regulates centrosome duplication. Downregulation of Plk1 in *Tsc1*^{-/-} MEFs by siRNA did not rescue the increased centrosome number phenotype. Finally, nocodazole-arrested *Tsc1*^{-/-} MEFs, but not *Tsc2*^{-/-} MEFs, have increased DNA content (>4N). Both phenotypes are rescued after pre-treatment with rapamycin.

RESULTS

Hamartin localizes to the centrosome

To determine hamartin's localization during mitosis, Cos7 cells were treated with nocodazole and fixed in paraformaldehyde. Immunofluorescence confocal microscopy showed that hamartin and the centrosomal marker γ -tubulin co-localize on the same plane of nocodazole-arrested cells (Fig. 1A). The centrosomal localization of hamartin was verified in HeLa cells (Fig. 1B). Pre-incubation of the anti-hamartin antibody (4) with the immunizing peptide completely removed the staining from the centrosomes (Fig. 1B). The centrosome staining was also observed with a commercially available hamartin antibody from Invitrogen (Carlsbad, CA, USA) (data not shown).

Centrosomal fractionation was used to confirm the immunofluorescence results. Centrosomes from nocodazole-arrested NIH3T3 cells were initially purified over a sucrose cushion and further fractionated by ultracentrifugation in a discontinuous sucrose gradient. Hamartin was present primarily in fractions 12–14 (Fig. 1C), which are enriched in centrosomes as indicated by the increase in γ -tubulin. Tuberin was also present in fractions 12–14, although the enrichment of tuberin in these fractions was less pronounced than hamartin or γ -tubulin.

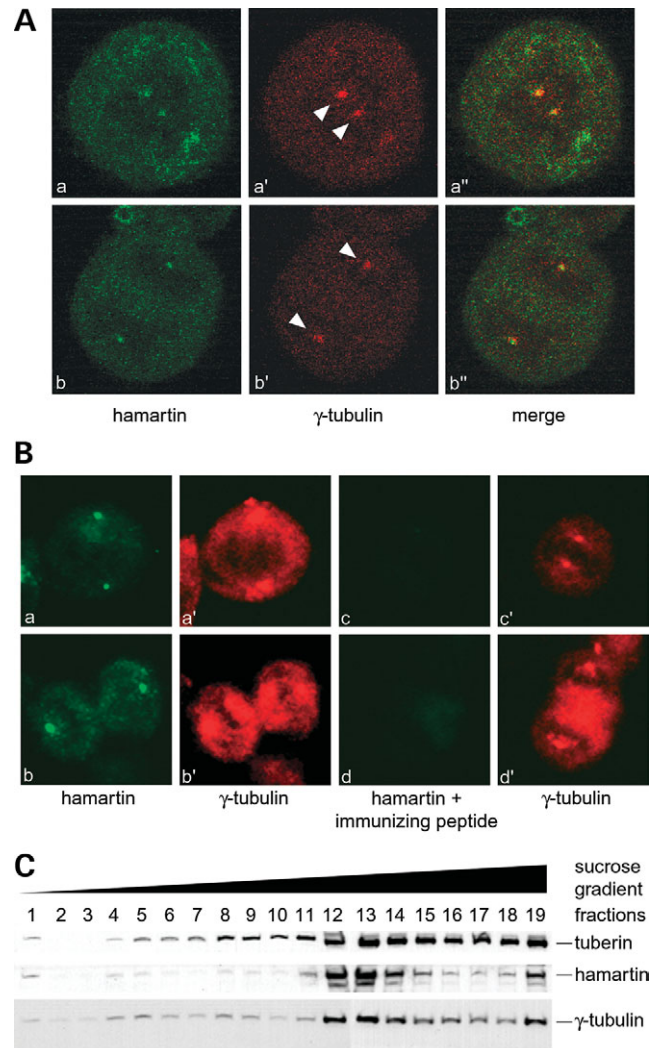


Figure 1. Hamartin localizes to the centrosome. (A) Cos7 cells were arrested in G₂/M with 70 ng/ml nocodazole for 18.5 h. Cells were fixed in paraformaldehyde, permeabilized with 0.5% Tween-20, stained with hamartin antibodies (a and b) and co-stained with γ -tubulin antibodies (a' and b'). The merged confocal images (a'' and b'') show that hamartin is co-localized with γ -tubulin at the centrosomes (arrowheads) during metaphase (a'') and telophase (b''). (B) HeLa cells were treated with nocodazole, stained in ice-cold methanol and permeabilized with 0.2% Triton X-100 in 1 \times PBS, then incubated with anti-hamartin (a and b) and anti- γ -tubulin antibodies (a', b', c' and d'). These antibodies stained the centrosome of metaphase and telophase cells (a and b, respectively). The immunostaining was abolished when the anti-hamartin antibody was pre-incubated with the immunizing peptide (c and d). (C) NIH3T3 cells were treated with nocodazole for 18.5 h, then with cytochalasin B for 90 min. Centrosome fractions were isolated by a discontinuous sucrose gradient, the proteins resolved in a 7.5% Tris-HCl SDS/PAGE and immunoblotted. Hamartin and tuberin co-fractionated with γ -tubulin (fractions 12–14).

Phospho-hamartin co-immunoprecipitates with endogenous Plk1

Previously we reported that hamartin is threonine-proline phosphorylated by CDC2/cyclin B1 during G₂/M arrest and during normal G₂/M progression (14). Three of the five potential CDC2/cyclin B1 phosphorylation sites on hamartin (S-T³¹⁰-P, S-S³³²-P and S-T¹⁰⁴⁷-P) match the binding motif for the PBD of the mitotic kinase Plk1 (21). Therefore, we

hypothesized that phosphorylated hamartin interacts with Plk1 during the G₂/M phase of the cell cycle. We found that endogenous Plk1 co-immunoprecipitates with endogenous hamartin and tuberin from nocodazole arrested HEK293 cells (Fig. 2A). To confirm the specificity of the interaction, we performed Plk1 immunoprecipitations from vehicle or nocodazole-treated HEK293 cells. Hamartin was present only in the Plk1 immunoprecipitates from nocodazole-treated cells (Fig. 2B). More importantly, the hamartin that co-immunoprecipitated with Plk1 had slower electrophoretic mobility, suggesting that Plk1 interacts exclusively with phosphorylated hamartin.

To confirm that the mobility shift of hamartin present in Plk1 immunoprecipitates is due to phosphorylation, myc-Plk1 was expressed in HEK293 cells, and the resulting myc immunoprecipitates were treated with calf intestinal alkaline phosphatase (CIAP). Treatment of the myc-Plk1 immunoprecipitates restored the normal electrophoretic mobility of hamartin (Fig. 2C), indicating that Plk1 interacts with a phosphorylated form of hamartin. Interestingly, CIAP treatment of the myc-Plk1 immunoprecipitates also increased the mobility of tuberin (Fig. 2C), demonstrating that the tuberin within the hamartin/Plk1 complex is also phosphorylated.

Plk1 interacts with phospho-hamartin independent of tuberin

To determine whether the Plk1/tuberin interaction is dependent on the hamartin/tuberin interaction, HisXpress-tagged hamartin was expressed in HEK293 cells either with wild-type tuberin or with mutant R611Q tuberin. R611Q is one of the most frequent mutations in TSC patients and does not interact with hamartin (22). Co-expression of TSC1 with TSC2-R611Q increased the interaction between hamartin and Plk1 when compared with co-expression of TSC1 with wild-type TSC2 (Fig. 3A, compare third and first lanes, respectively). These results suggest that the hamartin/Plk1 interaction is not dependent on the interaction of hamartin with tuberin. Plk1 co-immunoprecipitated with His-tagged R611Q tuberin to a lesser extent (Fig. 3A, fourth lane) compared with His-tagged wild-type tuberin (second lane). These results suggest that hamartin mediates the interaction between Plk1 and the hamartin/tuberin complex. Although Nellist *et al.* (22) previously found that tuberin-R611Q did not interact with hamartin, in our experiments a significant amount of hamartin was present in the His-tuberin-R611Q immunoprecipitates (Fig. 3A). This difference between our results and Nellist *et al.* likely reflect the much lower expression in the Nellist *et al.* study, compared to our expression levels in Figure 3A.

To confirm that Plk1 interacts with the hamartin/tuberin complex in a hamartin-dependent manner, we re-introduced hamartin in *Tsc1*^{-/-} MEFs and created stable cell lines. Expression levels of hamartin and tuberin in a vector-control *Tsc1*^{-/-} cell line (P2) and in two hamartin re-expressing cell lines (T3 and T9) are shown in Figure 3B. As reported previously (23), re-expression of hamartin increased the stability of tuberin. Tuberin was present in the Plk1 immunoprecipitates from hamartin-expressing clones T3 and T9 but not the vector-control clone P2 (Fig. 3C), indicating that the Plk1/tuberin interaction is not direct and is mediated by hamartin.

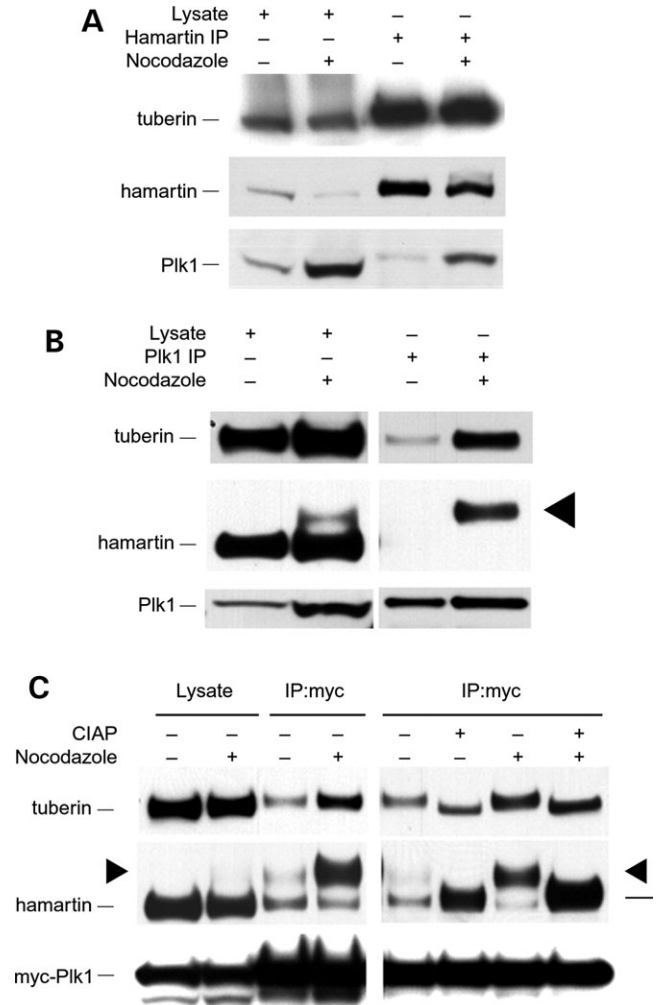


Figure 2. Plk1 interacts with phosphorylated hamartin. (A) HEK293 cells were treated with nocodazole (or vehicle control) for 18.5 h, lysed in PTY buffer, endogenous hamartin was immunoprecipitated and resolved in 3–8% Tris–acetate PAGE. The amount of Plk1 present in the hamartin immune complexes was increased in nocodazole-arrested cells. These data are representative of at least three independent experiments. (B) HEK293 cells were treated as in (A), endogenous Plk1 was immunoprecipitated and resolved in 3–8% Tris–acetate PAGE. Phosphorylated hamartin (arrowhead) co-immunoprecipitated with Plk1 only in the presence of nocodazole. These data are representative of three independent experiments. (C) HEK293 cells were transfected with myc-Plk1 and treated with nocodazole. Myc-immunoprecipitates were treated with CIAP and resolved in 3–8% Tris–acetate PAGE. Hamartin in untreated myc-Plk1 immunoprecipitates migrated more slowly (arrowhead). Treatment of the myc immunoprecipitates with CIAP restored the normal mobility of hamartin, indicating that the upshifted form of hamartin is phosphorylated. CIAP treatment increased the mobility of tuberin, indicating that the tuberin complexed with hamartin and Plk1 is also phosphorylated.

The N-terminus of hamartin binds Plk1

To identify the domains through which hamartin interacts with Plk1, HEK293 cells were transfected with His-tagged full-length TSC1 (amino acids 1–1164), N-terminal TSC1 (N-TSC1, amino acids 1–880) or C-terminal TSC1 (C-TSC1, amino acids 511–1164) (Fig. 4A and B). Plk1 co-immunoprecipitated with the full-length and N-terminal hamartin constructs (Fig. 4B), but not with the C-terminal

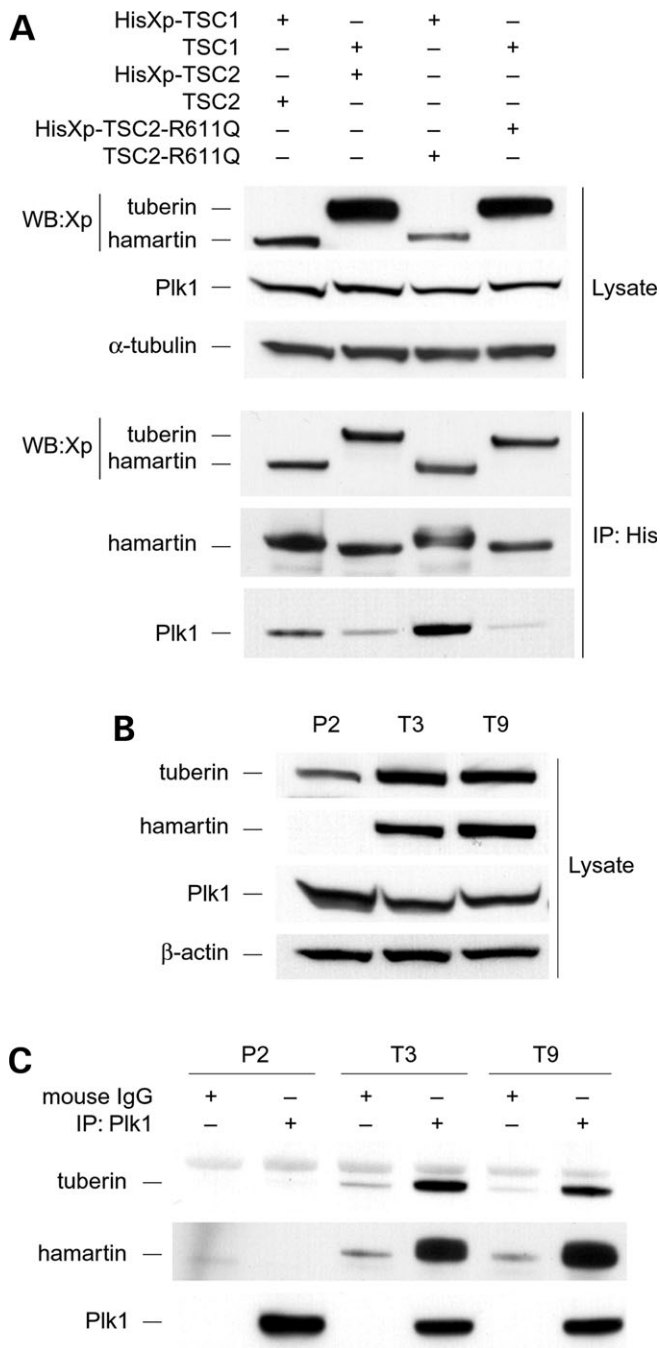


Figure 3. Plk1 interacts with phospho-hamartin independent of tuberlin. (A) HEK293 cells were transfected with HisXp-TSC1/TSC2, TSC1/HisXp-TSC2, HisXp-TSC1/TSC2-R611Q or TSC1/HisXp-TSC2-R611Q, then treated with nocodazole for 18.5 h. His immunoprecipitates were resolved in 4–12% Bis-Tris PAGE and immunoblotted with anti-Xpress, anti-Plk1 and anti-hamartin antibodies. Plk1 co-immunoprecipitated with HisXp-hamartin (first and third lanes). The amount of Plk1 in the immunoprecipitates was increased in cells expressing TSC2-R611Q. Immunoprecipitates of HisXp-tuberin or HisXp-tuberin-R611Q contained comparatively less Plk1 (second and fourth lanes). (B) Nocodazole-treated whole cell lysates from *Tsc1*^{-/-} MEFs with stable re-expression of hamartin (clones T3 and T9) and vector-control clone (P2) were immunoblotted for tuberlin, hamartin, Plk1 and β -actin as a loading control. (C) Endogenous Plk1 was immunoprecipitated from the MEF clones shown in (B). Hamartin co-immunoprecipitated with Plk1 from clones T3 and T9. Tuberlin was absent from the Plk1 immune complexes in the MEFs lacking hamartin (P2). Mouse IgG was used as a control.

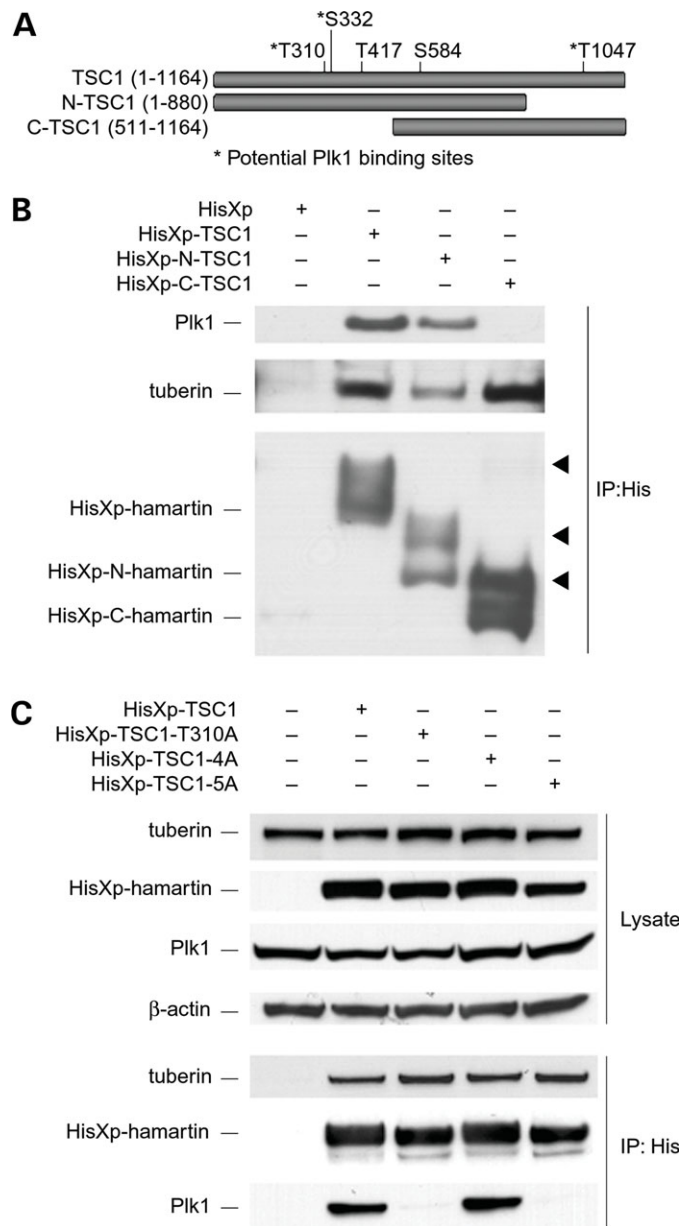


Figure 4. Hamartin residue T310 is required for Plk1 interaction. (A) Diagram of hamartin deletion constructs (N-TSC1, amino acids 1–880 and C-TSC1, amino acids 511–1164). Hamartin contains five potential CDC2/cyclin B1 phosphorylation sites (T310, S332, T417, S584 and T1047). Three of these sites (T310, S332 and T1047) are within potential Plk1 PBD-binding motifs. (B) HEK293 cells were transfected with HisXp, HisXp-TSC1, HisXp-N-TSC1 (amino acids 1–880) and HisXp-C-TSC1 (amino acids 511–1164), then treated with nocodazole for 18.5 h. His immunoprecipitates were resolved in 3–8% Tris-acetate PAGE and immunoblotted with antibodies to Plk1, Xpress and tuberlin. Endogenous Plk1 was present in the immunoprecipitates of full-length and N-terminal hamartin (second and third lanes), but not in the immunoprecipitates of C-terminal hamartin (fourth lane) or the vector control. All hamartin constructs appeared to be phosphorylated, resulting in upshifted forms (arrowheads). (C) HEK293 cells were transfected with HisXp-TSC1, HisXp-TSC1-T310A, His-TSC1-4A (S332A/T417A/S584A/T1047A quadruple mutant) or HisXp-TSC1-5A (T310A/S332A/T417A/S584A/T1047A quintuple mutant), then treated with nocodazole for 18.5 h. His immunoprecipitates were resolved in 4–12% Bis-Tris PAGE and immunoblotted for Xpress, tuberlin and Plk1. Endogenous Plk1 co-immunoprecipitated with wild-type TSC1 and TSC1-4A (second and fourth lanes), but not with TSC1-T310A (third lane), TSC1-5A (fifth lane) or vector control.

hamartin construct. Tuberin co-immunoprecipitated with all three hamartin constructs (Fig. 4B). These results suggest that the hamartin/Plk1 interaction is mediated by hamartin amino acids 1–510.

Hamartin residue T310 is responsible for the hamartin/Plk1 interaction

CDC2/cyclin B1 phosphorylates serine/threonine residues within both consensus (K/R-S/T-P-X-K/R) (24) and non-consensus motifs (S/T-P) (25). Hamartin contains a total of five potential CDC2/cyclin B1 sites: three consensus sites (predicted phosphorylation at residues T417, S584 and T1047) and two non-consensus sites (T310 and S332) (Fig. 4A). Of these sites, three (T310, S332 and T1047) are part of potential Plk1-binding motifs (15,20). The N-terminus of hamartin, which interacts with Plk1, contains two potential CDC2/cyclin B1 phosphorylation and Plk1 PBD-binding sites at residues T310 and S332. Amino acid T310 is within the most stringent consensus PBD-binding motif as defined by Elia *et al.* (20).

To identify the hamartin residues mediating binding to Plk1, three His-tagged non-phosphorylatable hamartin alanine mutants were created: a TSC1-T310A single mutant, TSC1-4A (S332A/T417A/S584A/T1047A) and TSC1-5A (T310A/S332A/T417A/S584A/T1047A). The hamartin alanine mutants were expressed in HEK293 cells and the cells arrested with nocodazole. We found that endogenous Plk1 co-immunoprecipitated with wild-type hamartin and TSC1-4A (Fig. 4C). In contrast, Plk1 did not co-immunoprecipitate with the hamartin mutants TSC1-5A or TSC1-T310A. These data suggest that hamartin T310 is a major determinant for Plk1 binding.

Hamartin expression negatively regulates Plk1 protein levels

Using western immunoblotting, we observed that Plk1 protein levels were decreased in *Tsc1*^{-/-} MEFs with stable hamartin re-introduction (clones T3 and T9), compared with the vector-control stable clone P2 (Fig. 3B). Similar results were seen in *Tsc1*^{-/-} MEFs which have 2.2-fold higher Plk1 expression than *Tsc1*^{+/+} cells (Fig. 5A). To verify that hamartin expression affects Plk1 protein levels, we used an RNAi approach. U2OS cells were transfected with siRNA for *TSC1*, *TSC2* and *PLK1*, and the protein levels were assayed by western immunoblotting. Silencing of *TSC1* or *TSC2* increased Plk1 protein levels in G₂/M-arrested cells by 2.4- and 1.9-fold, respectively (Fig. 5B). Silencing of *PLK1* slightly decreased the hamartin and tuberin protein levels.

RNAi-mediated Plk1 in U2OS cells decreased the phosphorylation of p70S6K at residue T389, ribosomal protein S6 at residues S235/S236 and 4E-BP1 at residue T70, both in nocodazole-arrested U2OS cells (Fig. 5B) and in asynchronous cells (data not shown).

Hamartin regulates centrosome number in an mTOR-dependent manner

Because Plk1 is implicated in centrosome maturation (26), we tested whether hamartin is required for maintenance of proper centrosome number. We found that 59.5% of *Tsc1*^{-/-} MEFs

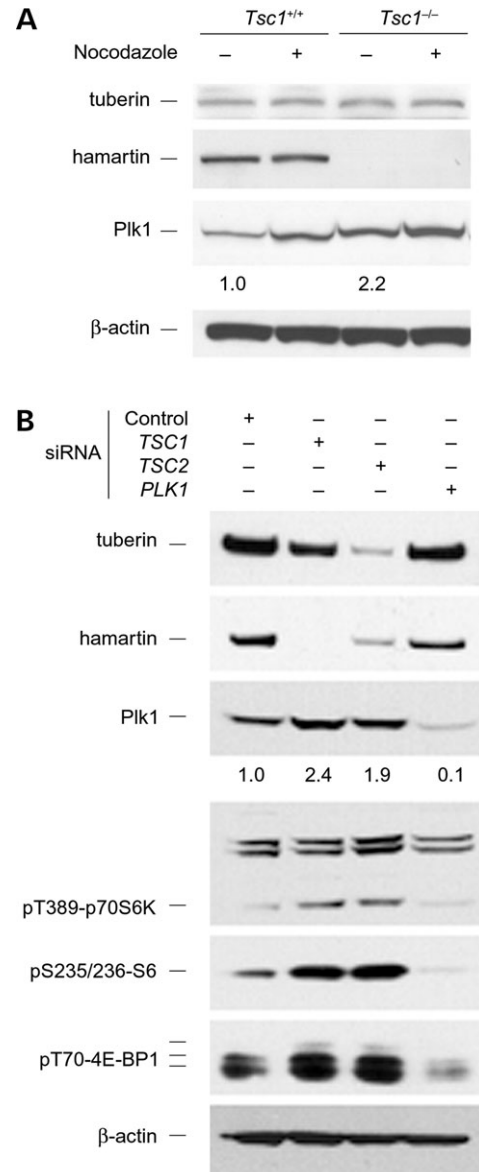


Figure 5. Plk1 expression is regulated by hamartin. (A) *Tsc1*^{+/+} and *Tsc1*^{-/-} MEFs were treated with nocodazole (or vehicle control) for 16 h, then lysed in PTY buffer. Lysates were resolved in 4–12% Bis-Tris PAGE and immunoblotted for hamartin, tuberin, Plk1 and β-actin (loading control). Densitometry values (arbitrary units) are indicated under the Plk1 immunoblot. (B) U2OS cells were transfected with control siRNA, *TSC1*, *TSC2* or *PLK1* siRNA. After 48 h, the cells were treated with nocodazole for 16 h, lysed in PTY buffer, proteins resolved in 4–12% Bis-Tris PAGE and immunoblotted for tuberin, hamartin, Plk1, pT389-p70S6K, pS235/236-S6, pT70-4E-BP1 and β-actin (loading control). Densitometry values (arbitrary units) are indicated under the Plk1 immunoblot. Silencing of Plk1 decreased the protein levels of hamartin and tuberin. *PLK1* siRNA decreased the phosphorylation of p70S6K, S6 and 4E-BP1. The additional bands above pT389-p70S6K represent cross-reactivity of the antibody with p85S6K.

have multiple (more than two) centrosomes, compared to 34.4% of *Tsc1*^{+/+} MEFs ($P < 0.05$, Fig. 6A and 6B). We hypothesized that the increased centrosome number was caused by the aberrant mTOR activation observed in *Tsc1*^{-/-} MEFs. Pre-treatment of *Tsc1*^{-/-} MEFs with 2 nM of the mTOR inhibitor rapamycin reduced the percentage of cells

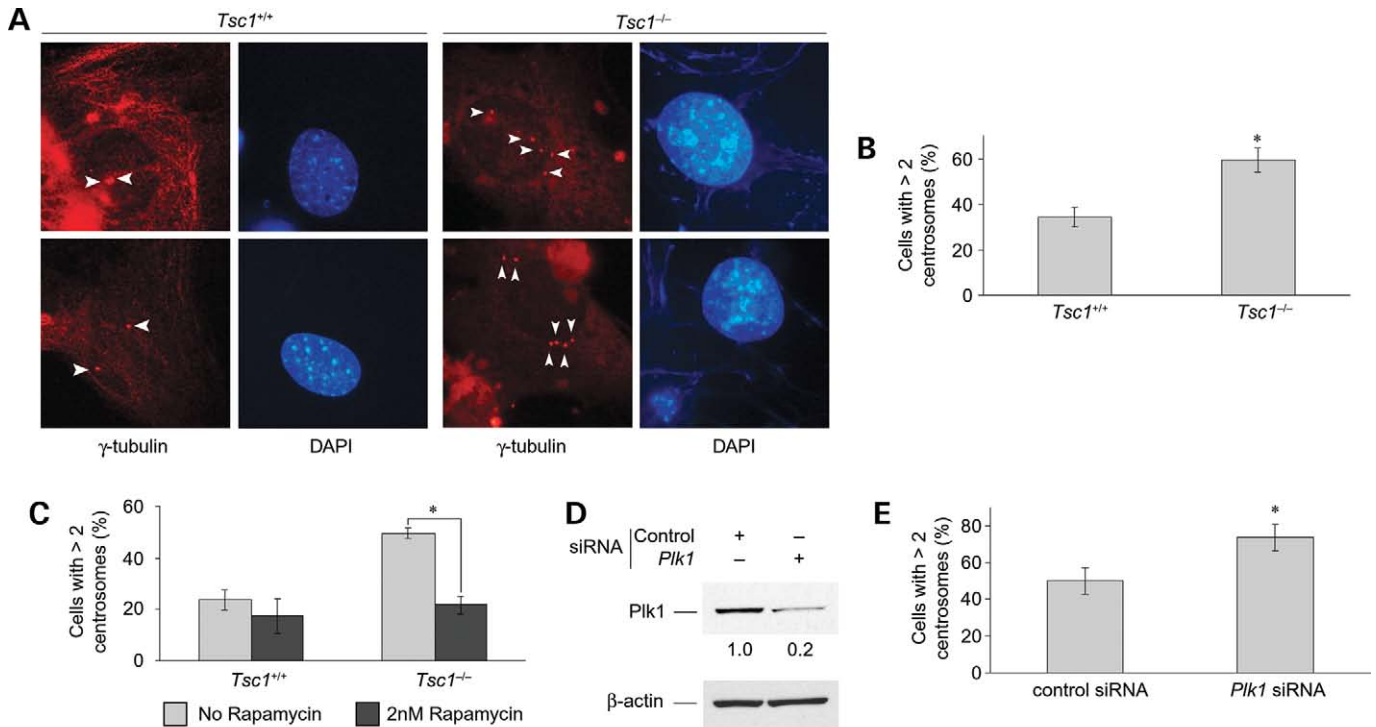


Figure 6. Hamartin-deficient MEFs have increased centrosome number which is rescued by rapamycin. (A) *Tsc1*^{+/+} and *Tsc1*^{-/-} MEFs were arrested in G₁/S with 500 μ M hydroxyurea for 40 h, fixed in methanol, stained for γ -tubulin and the nuclei counterstained with DAPI. Indirect immunofluorescence was used to observe the centrosomes (arrowheads). Multiple centrosomes are observed in the *Tsc1*^{-/-} MEFs. (B) Quantitation of the results from (A). Centrosomes were counted from more than 100 cells by two independent investigators blinded to the experimental conditions. Results are representative of three independent experiments. About 59.5% of *Tsc1*^{-/-} MEFs have multiple (more than two) centrosomes, compared with 34.4% of *Tsc1*^{+/+} MEFs (asterisk indicates statistical significance at $P < 0.05$). (C) *Tsc1*^{+/+} or *Tsc1*^{-/-} MEFs were pre-treated for 24 h with 2 nM rapamycin (closed boxes) or vehicle control, then arrested in G₁/S with 500 μ M hydroxyurea in the presence of rapamycin and centrosome number counted as in (B). Results are representative of three independent experiments. Multiple (more than two) centrosomes were observed in 21.8% of rapamycin-pre-treated *Tsc1*^{-/-} MEFs, compared with 49.6% of untreated cells (asterisk indicates statistical significance at $P < 0.05$). (D) *Tsc1*^{-/-} MEFs were transfected with 100 nM control or *Plk1* siRNA for 72 h. Densitometry values (arbitrary units) are indicated under the Plk1 immunoblot. Plk1 protein levels from *Plk1* siRNA-transfected *Tsc1*^{-/-} MEFs were 20% of the control siRNA-transfected cells. (E) *Tsc1*^{-/-} MEFs were transfected with 100 nM control or *Plk1* siRNA for 24 h, then arrested in G₁/S with 500 μ M hydroxyurea in the presence of siRNAs, fixed and stained as in (A) and the centrosome number counted from 300 cells. Results are averages of two independent experiments. About 73.7% of *Plk1* siRNA-transfected cells had multiple (more than two) centrosomes, compared with 50.1% of control siRNA-transfected cells (asterisk indicates statistical significance at $P < 0.05$). In all graphs, error bars represent standard deviation.

with multiple centrosomes from 49.6 to 21.8% (Fig. 6C, $P < 0.05$). In *Tsc1*^{+/+} MEFs, rapamycin pre-treatment had only a minimal effect, reducing the percentage of cells with multiple centrosomes from 23.7 to 17.4% ($P > 0.05$).

We then tested the hypothesis that the increase in the centrosome number observed in *Tsc1*^{-/-} MEFs is Plk1-dependent. *Plk1* siRNA reduced the Plk1 protein levels at 20% of control siRNA-transfected cells (Fig. 6D). Unexpectedly, 73.7% of *Tsc1*^{-/-} MEFs transfected with *Plk1* siRNA showed increased centrosome number, compared with 50.1% of control siRNA-transfected *Tsc1*^{-/-} MEFs (Fig. 6E, $P < 0.05$). These results suggest that the increase in centrosome number observed in hamartin-deficient cells is mTOR-dependent and Plk1-independent.

Hamartin-deficient cells have increased DNA content which is rescued by rapamycin

Centrosome multiplicity is associated with genomic instability and abnormal mitosis. As we observed that the *Tsc1*^{-/-}

MEFs have increased number of centrosomes, we asked whether they might also have mitotic defects. We found that 36.8% of nocodazole-arrested *Tsc1*^{-/-} MEFs have increased DNA content (>4 N), compared with 24.7% of *Tsc1*^{+/+} MEFs ($P < 0.01$, Fig. 7A and B). *Tsc1*^{-/-} MEFs released from the nocodazole block failed to progress to a normal cell cycle even 24 h after release (data not shown). Pre-treatment of the *Tsc1*^{-/-} MEFs with 2 nM rapamycin for 24 h prior to the nocodazole block was sufficient to rescue the increase in DNA content from 66.7 to 17.3% ($P < 0.05$, Fig. 7C and D). Treatment of the *Tsc1*^{-/-} MEFs with 2 nM rapamycin did not cause a G₁ arrest (G₁ fraction 50.9% in untreated cells versus 49.4% in treated cells, Fig. 7C).

We next asked whether the mitotic defect observed in the hamartin-deficient MEFs is also present in tuberin-deficient MEFs. About 46.6% of nocodazole-arrested *Tsc2*^{-/-} *p53*^{-/-} MEFs had increased (>4 N) DNA content, compared to 37.1% of *Tsc2*^{+/+} *p53*^{-/-} MEFs (Fig. 7E and F). This difference was not statistically significant ($P > 0.05$).

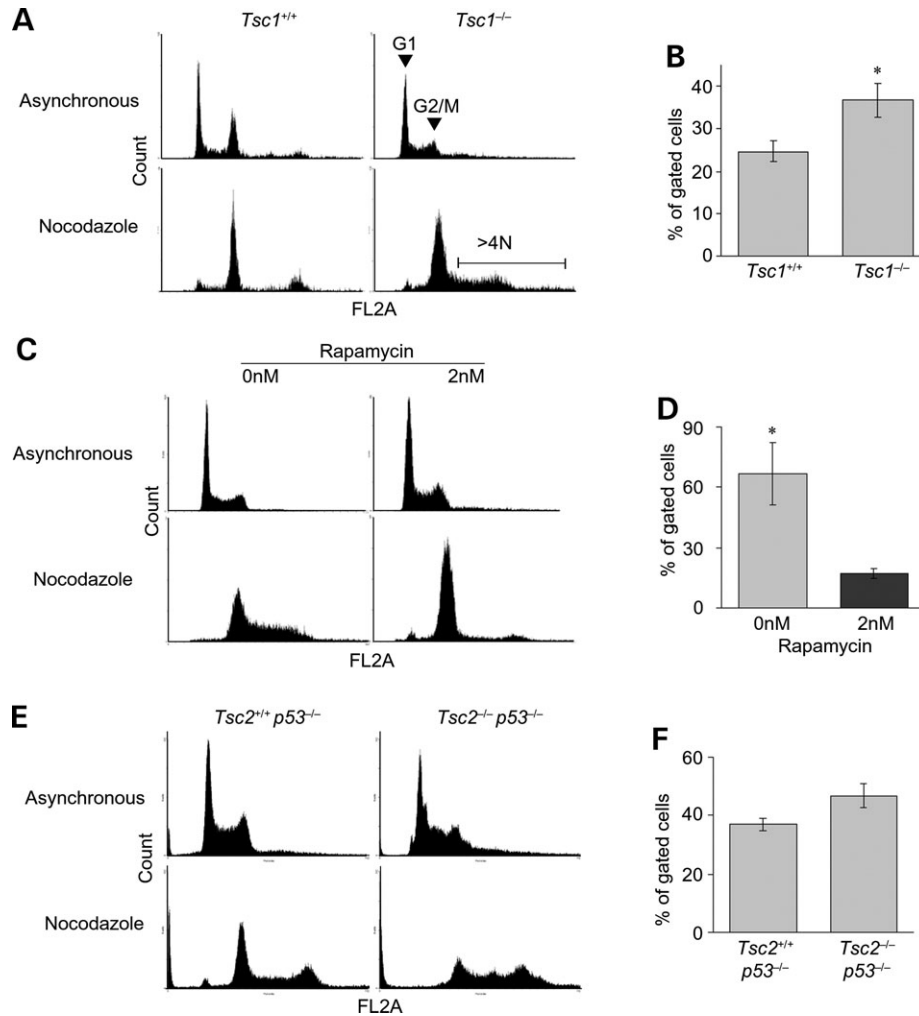


Figure 7. Hamartin-deficient MEFs have increased DNA content which is rescued by rapamycin. (A) Exponentially growing (asynchronous) *Tsc1*^{+/+} or *Tsc1*^{-/-} MEFs were treated with 70 ng/ml nocodazole for 16 h and the DNA content (FL2A) was measured by fluorescence-activated cell sorting (FACS). Arrowheads indicate the G₁ and G₂/M fractions of the cell population. The region of increased DNA content (>4N) was used for quantitation of the aneuploid fraction of cells. (B) Quantitation of the fraction of cells with increased DNA content. About 36.8% of *Tsc1*^{-/-} MEFs have >4N DNA content, compared with 24.7% of *Tsc1*^{+/+} MEFs (asterisk indicates statistical significance at $P < 0.01$). Averages of four independent experiments. (C) Exponentially growing (asynchronous) *Tsc1*^{-/-} MEFs were pre-treated with 2 nM rapamycin for 24 h, then treated with 70 ng/ml nocodazole for 16 h in the presence of rapamycin and subjected to FACS analysis. (D) About 66.7% of untreated *Tsc1*^{-/-} MEFs have >4N DNA content, compared with 17.3% of rapamycin-treated *Tsc1*^{-/-} MEFs (asterisk indicates statistical significance at $P < 0.05$). Averages of three independent experiments. (E) Exponentially growing (asynchronous) *Tsc2*^{+/+} *p53*^{-/-} or *Tsc2*^{-/-} *p53*^{-/-} MEFs were treated with 70 ng/ml nocodazole for 16 h, then subjected to FACS analysis. (F) About 46.6% of nocodazole-treated *Tsc2*^{-/-} *p53*^{-/-} MEFs had increased (>4N) DNA content, compared with 37.1% of *Tsc2*^{+/+} *p53*^{-/-} MEFs ($P > 0.05$). Results are averages of two independent experiments. In all graphs, error bars represent standard deviations.

DISCUSSION

Relatively little is known about the function and regulation of hamartin, especially when compared with the rapidly expanding knowledge of tuberlin's function and regulation. We report here that hamartin is centrosomally localized and that Plk1 is a novel interacting partner for the hamartin/tuberlin complex. Interaction of the hamartin/tuberlin complex with Plk1 appears to be mediated by phosphorylated hamartin, as tuberlin is not present in Plk1 immunoprecipitates from *Tsc1*^{-/-} MEFs. We found that the N-terminus of hamartin (amino acids 1–880) interacts strongly with Plk1, whereas the C-terminus (amino acids 511–1164) does not, indicating that the hamartin/Plk1 interaction domain resides within the

first 510 amino acids of hamartin. Both constructs interact with tuberlin, suggesting either that hamartin has two distinct tuberlin-interaction domains (amino acids 1–510 and 881–1164), or that the tuberlin-interaction domain lies within hamartin amino acids 511–880. Our findings complement the yeast two-hybrid work of Hodges *et al.* (6), which suggested that hamartin contains multiple tuberlin-interaction domains at the N-terminus (residues 1–430). Hamartin's C-terminus interacted weakly with tuberlin in the yeast system, but strongly in the mammalian cells. To our knowledge, these yeast two-hybrid results have never been validated in mammalian cells. Additional work is needed to define the domains through which hamartin interacts with tuberlin in mammalian cells.

To identify the residues responsible for the hamartin/Plk1 interaction, we created non-phosphorylatable alanine mutants of hamartin at the potential CDC2/cyclin B1 phosphorylation sites T310, S332, T417, S584 and T1047. We found that a single alanine mutation at hamartin residue T310 was sufficient to disrupt the hamartin/Plk1 interaction, suggesting that Plk1 binds hamartin when it is phosphorylated at threonine 310. A quadruple non-phosphorylatable hamartin alanine mutant (S332A/T417A/S584A/T1047A) did not affect the interaction with Plk1. This indicates that phosphorylation at these four sites is not required for Plk1 interaction nor are they required as priming phosphorylation events for T310 phosphorylation. Tuberin is present in the immune complexes of the wild-type and all hamartin mutants suggesting that overall folding and stability of the protein was maintained and the hamartin/tuberin complex is not influenced by the hamartin/Plk1 interaction.

We found that Plk1 protein levels increased in *Tsc1*^{-/-} MEFs, and after siRNA silencing of either *TSC1* or *TSC2*, indicating that loss of hamartin or tuberin leads to increased expression or decreased degradation of Plk1. Plk1 expression is often increased in cancer (27–29), and a specific Plk1 inhibitor was recently reported (30). The ubiquitin ligase CHFR (checkpoint with forkhead and ring finger domains) is believed to regulate the proteasome-dependent degradation of Plk1 (31), although the exact molecular mechanisms for the regulation of Plk1 levels during the cell cycle are not completely understood. Additional studies are needed to identify the mechanism of the increased Plk1 protein in hamartin-null cells and to determine whether Plk1 inhibition has potential benefits in the treatment of TSC.

Plk1 is pivotal for centrosome maturation (32), and depletion of Plk1 by siRNA has been reported to decrease the number of centrosomes in G₁/S phase arrested cells (26). Our finding that hamartin localizes to the centrosome and that Plk1 interacts with the hamartin/tuberin complex suggests that hamartin may play a functional role in the regulation of centrosome maturation and/or mitotic progression. In agreement with this hypothesis, we found that the *Tsc1*^{-/-} MEFs have increased percentage of cells with multiple centrosomes, compared with *Tsc1*^{+/+} MEFs. Pre-treatment of the *Tsc1*^{-/-} MEFs with low doses of rapamycin rescued this phenotype, suggesting that centrosome duplication is regulated by the hamartin–tuberin–mTOR pathway. To our surprise, siRNA-mediated silencing of *Plk1* in the hamartin-deficient MEFs not only failed to decrease, but also *increased* the percentage of cells with multiple centrosomes. These results indicate that the increased centrosome number observed in the *Tsc1*^{-/-} MEFs is Plk1-independent. The increase in centrosome number after Plk1 siRNA was unexpected because of the work of Liu and Erikson (26) who demonstrated that RNAi-mediated inhibition of *PLK1* in U2OS cells decreases the multiplicity of centrosomes. This could mean that centrosome amplification is controlled through different mechanisms in different cell types.

We also found that nocodazole-arrested *Tsc1*^{-/-} MEFs have increased fraction of cells with >4 N DNA content, a phenotype that is rescued after pre-treatment with rapamycin. In *Tsc2*^{-/-} *p53*^{-/-} MEFs, we observed an increase in the >4 N DNA content fraction of cells compared with *Tsc2*^{+/+}

p53^{-/-} MEFs; however this increase was not statistically significant. At this point, it is unclear whether the differences in mitotic defects between the *Tsc1*^{-/-} and the *Tsc2*^{-/-} *p53*^{-/-} MEFs represent separable functions of hamartin and tuberin or p53 dependence. Expression of a Plk1 kinase dead mutant (K82M) or a deletion mutant that does not contain the kinase domain (Plk1ΔN) causes mitotic arrest with increase in the >4 N DNA content and failure of cytokinesis (19), apparently caused by a spindle checkpoint defect. It is possible that the >4 N DNA content phenotype we observed in the hamartin-null MEFs involves similar pathways to bypass a spindle checkpoint.

At least two other tumor suppressor genes (BRCA1 and p53), both of which function in part to maintain genome stability, have centrosomal localization (33). Moreover, Plk1 phosphorylates the DNA damage checkpoint proteins Chk2 (34) and BRCA1 (35,36), suggesting that the centrosomes play a significant role in maintenance of genomic stability through the cross-talk of spindle and DNA damage checkpoint pathways with those of mitotic progression (37). Whether hamartin regulates genomic stability is not known. *dTsc1* and *dTsc2* mutant *Drosophila* cells have multiple cell cycle defects, including elevated levels of mitotic cyclins, even in post-mitotic cells (38). The underlying mechanisms are not completely understood. TSC patient-derived cells exhibit prolonged S phase of the cell cycle (39). Although not extensively studied, there are numerous reports of chromosomal instability in TSC tumors, including multiple complex translocations (40–42), trisomies (43) and chromosome losses (44). Whether these defects are linked to the hamartin/Plk1 interaction is not known yet.

Mitotic progression is a complex biological process involving the co-ordinated activation, inactivation and changes in expression of key proteins. During late G₂, Plk1 directly phosphorylates and activates the phosphatase CDC25C, which in turn dephosphorylates and activates CDC2. Cyclin B1 expression increases in late G₂ and the formation of CDC2/cyclin B1 complexes allows mitotic entry. We propose a model in which the interaction between the hamartin/tuberin complex and Plk1 regulates mitotic protein synthesis locally (Fig. 8). Local protein translation is believed to be important in all organisms, with *Drosophila* and *Xenopus* the most studied and understood (reviewed in 45). For example, in *Xenopus* embryos, centrosomally localized protein translation of cyclin B1 seems to be regulated by cytoplasmic polyadenylation element-binding protein and maskin, impacting the mitotic apparatus and cell division (46). In our proposed model, the interaction between Plk1 and the hamartin/tuberin complex regulates local mTOR activity, resulting in increased mRNA translation of cyclin B1 and other key proteins in or around the centrosomes, thus promoting mitotic entry.

MATERIALS AND METHODS

Cloning and site-directed mutagenesis

Wild-type human *TSC1* coding region was subcloned in pcDNA3.1 +/His (Invitrogen) and the pMSCVneo retroviral vector (BD Biosciences, Mountain View, CA, USA). Site-directed mutagenesis was performed using the QuikChange

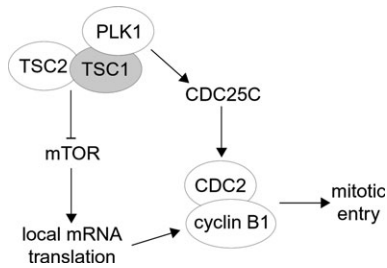


Figure 8. Proposed model for the role of Plk1/hamartin/tuberin interaction in regulation of local protein synthesis. The Plk1 interaction with hamartin regulates mTOR-dependent local protein synthesis in or around the centrosomes, with consequent centrosome duplication and increase in cyclin B1 mRNA translation during late G₂. Simultaneously, Plk1 activates CDC2 via the direct phosphorylation of CDC25C. The formation of CDC2/cyclin B1 complex allows mitotic entry.

site-directed mutagenesis kit (Stratagene, La Jolla, CA, USA). *PLK1* cDNA (IMAGE clone 2822226, ATCC, Manassas, VA, USA) was sub-cloned in pCMV/Tag3 vector (Stratagene) using high fidelity PCR. All cDNAs were fully sequence-confirmed.

Cell treatments and generation of stable cell lines

HEK293, Cos7, HeLa and U2OS cells (all from ATCC) were cultured in Dulbecco's modified Eagle's medium (DMEM), 10% fetal bovine serum, 100 U/ml penicillin, 100 µg/ml streptomycin and 2 mM L-glutamine. NIH3T3 cells (ATCC) were cultured in DMEM with 10% calf serum, 100 U/ml penicillin, 100 µg/ml streptomycin and 2 mM L-glutamine. *Tsc1*^{+/+}, *Tsc1*^{-/-}, *Tsc2*^{+/+} *p53*^{-/-} and *Tsc2*^{-/-} *p53*^{-/-} MEFs (the gift of Dr David Kwiatkowski, Brigham and Women's Hospital, Boston, MA, USA) (47) were cultured in DMEM, 10% fetal bovine serum, 100 U/ml penicillin, 100 µg/ml streptomycin, 2 mM L-glutamine and 100 µM non-essential amino acids. *Tsc1*^{-/-} MEFs were retrovirally transduced with human *TSC1*/pMSCVneo as previously described (48). Stable clones were selected over 2 weeks by addition of 500 µg/ml G418 in the growth medium. Expression of hamartin was assayed by western immunoblotting.

Cells were arrested in G₂/M using 70 ng/ml nocodazole (Sigma, St Louis, MO, USA) for 18.5 h. For quantitation of centrosome number, cells were arrested in G₁/S using 500 µM hydroxyurea (Sigma) for 40 h. Where indicated, cells were treated with 2 nM rapamycin (Biomol, Plymouth Meeting, PA, USA) for 24 h.

Transfections were performed using Lipofectamine 2000 (Invitrogen). RNA silencing was achieved using human *TSC1*, *TSC2* or *PLK1* or mouse *Plk1* SMARTPool siRNAs (Dharmacon, Lafayette, CO, USA) at a final concentration of 100 nM. siRNAs were delivered to the cells using Transit-TKO transfection reagent (Mirus Bio Corporation, Madison, WI, USA).

Antibodies

Immunoprecipitations were performed with anti-hamartin, anti-Plk1 (Invitrogen) or anti-TetraHis (Qiagen, Valencia,

CA, USA) antibodies. Rabbit or mouse IgG (Santa Cruz Biotechnology, Santa Cruz, CA, USA) was used as control. Western immunoblotting was performed with anti-hamartin, anti-Plk1, anti-Xpress (Invitrogen), anti-tuberin C20 (Santa Cruz Biotechnology), anti-β-actin (Sigma) and anti-pS235/236-S6, anti-pT389-p70S6K and anti-pT70-4E-BP1 (Cell Signaling, Beverly, MA, USA). Immunofluorescence was performed with anti-hamartin (4) (Invitrogen) and anti-γ-tubulin (Sigma).

Immunofluorescence

Cells were plated on cover slips, fixed with either 4% paraformaldehyde (Electron Microscopy Sciences, Hatfield, PA, USA) in 1 × phosphate-buffered saline (PBS) or ice-cold methanol (Sigma) for 10 min at room temperature, permeabilized with 0.2% Triton X-100 in 1 × PBS and stained with the primary antibodies in blocking buffer (1 × PBS, 3% BSA, 0.2% Triton X-100). Secondary antibodies were conjugated with either AlexaFluor488 or AlexaFluor594 (Invitrogen). The nuclei were counterstained with 4',6-diamidino-2-phenylindole dihydrochloride (DAPI) (Sigma). Images were obtained using either a DXM1000 digital camera (Nikon, Tokyo, Japan) or an MRC600 confocal microscope (Bio-Rad, Hercules, CA, USA).

To determine centrosome number, cells were arrested in G₁/S with 500 µM hydroxyurea (Sigma) for 40 h, fixed in methanol and stained for γ-tubulin (Sigma).

Sucrose gradient fractionation

NIH3T3 cells were used to isolate centrosomes as previously described (49). Cells were grown on five 150 mm plates, treated with 70 ng/ml nocodazole for 18.5 h, then with cytochalasin B (Sigma) for 90 min prior to lysis. Cells were washed consecutively in the following solutions: 1 × PBS, 0.1 × PBS/8% sucrose and 8% sucrose. Cells were lysed in 7 ml of sucrose fractionation buffer [1 mM Tris-HCl pH 8, 0.5% Triton X-100, 0.1% β-mercaptoethanol, 50 µM PMSF, 1 mM Na₃O₄V, protease and phosphatase inhibitor cocktails (Sigma)]. After cell debris was removed by centrifugation, the supernatant was filtered through a 40 µm pore diameter nylon mesh, placed on top of a 1 ml 60% sucrose cushion and centrifuged at 12 000 r.p.m. for 40 min at 4°C in an HB-4 swing-bucket rotor (Sorvall, Asheville, NC, USA). All but 2 ml above the sucrose cushion were removed and discarded. The remaining lysate was mixed with the sucrose cushion to make a 20% sucrose solution with enriched centrosomes. The enriched centrosome lysate was placed on top of a discontinuous sucrose gradient range of 40, 50, and 70% sucrose in (10 mM PIPES pH 6.8, 1 mM EDTA, 0.1% Triton X-100, 0.1% β-mercaptoethanol). The gradient was centrifuged at 25 000 r.p.m. for 80 min at 4°C in an SW50.1 swing-bucket ultracentrifuge rotor (Beckman-Coulter, Fullerton, CA, USA). Fractions (250 µl each) were collected from the bottom up and washed with 10 mM PIPES pH 7.2. The fractions were centrifuged at 14 000 r.p.m. at 4°C, the pellets resuspended in 40 µl of SDS loading buffer and analyzed by SDS/PAGE and western immunoblotting.

Immunoblotting and immunoprecipitation

Cells were lysed in PTY buffer (50 mM HEPES, 50 mM NaCl, 5 mM EDTA, 1% Triton X-100, 50 mM NaF, 10 mM Na₄P₂O₇, 1 mM Na₃O₄V, 10 µg/ml phenylmethanesulfonyl fluoride) supplemented with protease and phosphatase inhibitor cocktails (Sigma). Protein concentration was determined by the Bradford method (Bio-Rad). Twenty-five micrograms of total lysate were resolved in 7.5 or 4–20% Tris–HCl (Bio-Rad), 3–8% Tris–Acetate or 4–12% Bis-Tris (Invitrogen) PAGE gels, then transferred to Immobilon-P membranes (Millipore, Billerica, MA, USA).

One milligram of total protein cell lysate was used for each immunoprecipitation. Five micrograms of antibody or IgG control was added to each sample and rotated at 4°C for 1 h. Fifty microlitres of Protein-A agarose beads (Invitrogen) were added to each sample and rotated at 4°C overnight. For myc immunoprecipitation, anti-myc-conjugated agarose beads (BD Biosciences) were incubated with lysate overnight. The beads were washed three times with 500 µl PTY buffer. Forty microlitres of SDS loading buffer was added to each sample. Twenty microlitres of each sample was analyzed by PAGE and western immunoblotting.

For phosphatase treatment of the immunoprecipitates, the agarose beads were washed three times with PTY buffer, three times with dephosphorylation buffer (50 mM Tris–HCl pH 7.5, 1 mM MgCl₂) then incubated in 100 µl dephosphorylation buffer for 10 min at 37°C. Thirty units of CIAP (Amersham Biosciences, Piscataway, NJ, USA) was added in each sample and incubated for an additional 30 min at 37°C. The beads were washed three times with dephosphorylation buffer, resuspended in 40 µl of loading buffer and analyzed by PAGE and western immunoblotting.

Fluorescence activated cell sorting

Exponentially growing cells were treated as indicated, trypsinized, washed once in ice-cold growth medium and once in 1 × PBS and fixed overnight in 1 ml 70% ethanol at –20°C. Cells were washed once in 1 × PBS and stained in (70 µM propidium iodide, 30 mM sodium citrate pH 7.0, 10 mg/ml RNase A) at 37°C for 30 min. Flow cytometry analysis was performed using a Becton-Dickinson FACScan machine and CellQUEST DNA Acquisition software.

ACKNOWLEDGEMENTS

We are grateful to Dr David Kwiatkowski (Brigham and Women's Hospital, Boston, MA, USA) for providing the *Tsc1*^{+/+}, *Tsc1*^{-/-}, *Tsc2*^{+/+} *p53*^{-/-} and *Tsc2*^{-/-} *p53*^{-/-} MEFs and to Drs Erica Golemis and Jonathan Chernoff for critical review of this manuscript. We thank the Fox Chase Cancer Center Cell Imaging Facility for their assistance with confocal microscopy. Funding was provided by The LAM Foundation (Cincinnati, OH, USA), the Tuberous Sclerosis Alliance (Silver Spring, MD, USA) and the NIH (DK 51052).

Conflict of Interest statement. None declared.

REFERENCES

- Gomez, M., Sampson, J.R. and Whittemore, V.H. (1999) *Tuberous Sclerosis Complex*, 3rd edn. Oxford University Press, New York.
- The European Chromosome 16 Tuberous Sclerosis Consortium (1993) Identification and characterization of the tuberous sclerosis gene on chromosome 16. *Cell*, **75**, 1305–1315.
- van Slegtenhorst, M., de Hoogt, R., Hermans, C., Nellist, M., Janssen, B., Verhoef, S., Lindhout, D., van den Ouweland, A., Halley, D., Young, J. *et al.* (1997) Identification of the tuberous sclerosis gene *TSC1* on chromosome 9q34. *Science*, **277**, 805–808.
- Plank, T.L., Yeung, R.S. and Henske, E.P. (1998) Hamartin, the product of the tuberous sclerosis 1 (*TSC1*) gene, interacts with tuberin and appears to be localized to cytoplasmic vesicles. *Cancer Res.*, **58**, 4766–4770.
- van Slegtenhorst, M., Nellist, M., Nagelkerken, B., Cheadle, J., Snell, R., van den Ouweland, A., Reuser, A., Sampson, J., Halley, D. and van der Sluijs, P. (1998) Interaction between hamartin and tuberin, the *TSC1* and *TSC2* gene products. *Hum. Mol. Genet.*, **7**, 1053–1057.
- Hodges, A.K., Li, S., Maynard, J., Parry, L., Braverman, R., Cheadle, J.P., DeClue, J.E. and Sampson, J.R. (2001) Pathological mutations in *TSC1* and *TSC2* disrupt the interaction between hamartin and tuberin. *Hum. Mol. Genet.*, **10**, 2899–2905.
- Garami, A., Zwartkruis, F.J., Nobukuni, T., Joaquin, M., Roccio, M., Stocker, H., Kozma, S.C., Hafen, E., Bos, J.L. and Thomas, G. (2003) Insulin activation of Rheb, a mediator of mTOR/S6K/4E-BP signaling, is inhibited by *TSC1* and 2. *Mol. Cell*, **11**, 1457–1466.
- Castro, A.F., Rebhun, J.F., Clark, G.J. and Quilliam, L.A. (2003) Rheb binds tuberous sclerosis complex 2 (*TSC2*) and promotes S6 kinase activation in a rapamycin- and farnesylation-dependent manner. *J. Biol. Chem.*, **278**, 32493–32496.
- Miloloza, A., Rosner, M., Nellist, M., Halley, D., Bernaschek, G. and Hengstschlager, M. (2000) The *TSC1* gene product, hamartin, negatively regulates cell proliferation. *Hum. Mol. Genet.*, **9**, 1721–1727.
- Soucek, T., Pusch, O., Wienecke, R., DeClue, J.E. and Hengstschlager, M. (1997) Role of the tuberous sclerosis gene-2 product in cell cycle control. Loss of the tuberous sclerosis gene-2 induces quiescent cells to enter S phase. *J. Biol. Chem.*, **272**, 29301–29308.
- Miloloza, A., Kubista, M., Rosner, M. and Hengstschlager, M. (2002) Evidence for separable functions of tuberous sclerosis gene products in mammalian cell cycle regulation. *J. Neuropathol. Exp. Neurol.*, **61**, 154–163.
- Rosner, M. and Hengstschlager, M. (2004) Tuberin Binds p27 and Negatively Regulates Its Interaction with the SCF Component Skp2. *J. Biol. Chem.*, **279**, 48707–48715.
- Soucek, T., Yeung, R.S. and Hengstschlager, M. (1998) Inactivation of the cyclin-dependent kinase inhibitor p27 upon loss of the tuberous sclerosis complex gene-2. *Proc. Natl Acad. Sci. USA*, **95**, 15653–15658.
- Astrinidis, A., Senapedis, W., Coleman, T.R. and Henske, E.P. (2003) Cell cycle-regulated phosphorylation of hamartin, the product of the tuberous sclerosis complex 1 gene, by cyclin-dependent kinase 1/cyclin B. *J. Biol. Chem.*, **278**, 51372–51379.
- Elia, A.E., Cantley, L.C. and Yaffe, M.B. (2003) Proteomic screen finds pSer/pThr-binding domain localizing Plk1 to mitotic substrates. *Science*, **299**, 1228–1231.
- Golsteyn, R.M., Mundt, K.E., Fry, A.M. and Nigg, E.A. (1995) Cell cycle regulation of the activity and subcellular localization of Plk1, a human protein kinase implicated in mitotic spindle function. *J. Cell Biol.*, **129**, 1617–1628.
- Arnaud, L., Pines, J. and Nigg, E.A. (1998) GFP tagging reveals human polo-like kinase 1 at the kinetochore/centromere region of mitotic chromosomes. *Chromosoma*, **107**, 424–429.
- Takai, N., Hamanaka, R., Yoshimatsu, J. and Miyakawa, I. (2005) Polo-like kinases (Plks) and cancer. *Oncogene*, **24**, 287–291.
- Seong, Y.S., Kamijo, K., Lee, J.S., Fernandez, E., Kuriyama, R., Miki, T. and Lee, K.S. (2002) A spindle checkpoint arrest and a cytokinesis failure by the dominant-negative polo-box domain of Plk1 in U-2 OS cells. *J. Biol. Chem.*, **277**, 32282–32293.
- Elia, A.E., Rellos, P., Haire, L.F., Chao, J.W., Ivins, F.J., Hoepker, K., Mohammad, D., Cantley, L.C., Smerdon, S.J. and Yaffe, M.B. (2003) The molecular basis for phosphodependent substrate targeting and regulation of Plks by the polo-box domain. *Cell*, **115**, 83–95.
- Lowery, D.W., Mohammad, D.H., Elia, A.E. and Yaffe, M.B. (2004) The polo-box domain: a molecular integrator of mitotic kinase cascades and polo-like kinase function. *Cell Cycle*, **3**, 128–131.

22. Nellist, M., Verhaaf, B., Goedbloed, M.A., Reuser, A.J., van den Ouweland, A.M. and Halley, D.J. (2001) TSC2 missense mutations inhibit tuberin phosphorylation and prevent formation of the tuberin-hamartin complex. *Hum. Mol. Genet.*, **10**, 2889–2898.
23. Benvenuto, G., Li, S., Brown, S.J., Braverman, R., Vass, W.C., Cheadle, J.P., Halley, D.J., Sampson, J.R., Wienecke, R. and DeClue, J.E. (2000) The tuberous sclerosis-1 (*TSC1*) gene product hamartin suppresses cell growth and augments the expression of the TSC2 product tuberin by inhibiting its ubiquitination. *Oncogene*, **19**, 6306–6316.
24. Songyang, Z., Blechner, S., Hoagland, N., Hoekstra, M.F., Piwnicka-Worms, H. and Cantley, L.C. (1994) Use of an oriented peptide library to determine the optimal substrates of protein kinases. *Curr. Biol.*, **4**, 973–982.
25. Shah, O.J., Ghosh, S. and Hunter, T. (2003) Mitotic regulation of ribosomal S6 kinase 1 involves Ser/Thr, Pro phosphorylation of consensus and non-consensus sites by Cdc2. *J. Biol. Chem.*, **278**, 16433–16442.
26. Liu, X. and Erikson, R.L. (2002) Activation of Cdc2/cyclin B and inhibition of centrosome amplification in cells depleted of Plk1 by siRNA. *Proc. Natl Acad. Sci. USA*, **99**, 8672–8676.
27. Weichert, W., Schmidt, M., Gekeler, V., Denkert, C., Stephan, C., Jung, K., Loening, S., Dietel, M. and Kristiansen, G. (2004) Polo-like kinase 1 is overexpressed in prostate cancer and linked to higher tumor grades. *Prostate*, **60**, 240–245.
28. Gray, P.J., Jr, Bearss, D.J., Han, H., Nagle, R., Tsao, M.S., Dean, N. and Von Hoff, D.D. (2004) Identification of human polo-like kinase 1 as a potential therapeutic target in pancreatic cancer. *Mol. Cancer Ther.*, **3**, 641–646.
29. Ahmad, N. (2004) Polo-like kinase (Plk) 1: a novel target for the treatment of prostate cancer. *FASEB J.*, **18**, 5–7.
30. Gumireddy, K., Reddy, M.V., Cosenza, S.C., Nathan, R.B., Baker, S.J., Papathi, N., Jiang, J., Holland, J. and Reddy, E.P. (2005) ON01910, a non-ATP-competitive small molecule inhibitor of Plk1, is a potent anticancer agent. *Cancer Cell*, **7**, 275–286.
31. Kang, D., Chen, J., Wong, J. and Fang, G. (2002) The checkpoint protein Chfr is a ligase that ubiquitinates Plk1 and inhibits Cdc2 at the G2 to M transition. *J Cell Biol*, **156**, 249–259.
32. Lane, H.A. and Nigg, E.A. (1996) Antibody microinjection reveals an essential role for human polo-like kinase 1 (Plk1) in the functional maturation of mitotic centrosomes. *J. Cell Biol.*, **135**, 1701–1713.
33. Fisk, H.A., Mattison, C.P. and Winey, M. (2002) Centrosomes and tumour suppressors. *Curr. Opin. Cell Biol.*, **14**, 700–705.
34. Tsvetkov, L., Xu, X., Li, J. and Stern, D.F. (2003) Polo-like kinase 1 and Chk2 interact and co-localize to centrosomes and the midbody. *J. Biol. Chem.*, **278**, 8468–8475.
35. Lin, H.R., Ting, N.S., Qin, J. and Lee, W.H. (2003) M phase-specific phosphorylation of BRCA2 by polo-like kinase 1 correlates with the dissociation of the BRCA2-P/CAF complex. *J. Biol. Chem.*, **278**, 35979–35987.
36. Lee, M., Daniels, M.J. and Venkitaraman, A.R. (2004) Phosphorylation of BRCA2 by the polo-like kinase Plk1 is regulated by DNA damage and mitotic progression. *Oncogene*, **23**, 865–872.
37. Kramer, A., Lukas, J. and Bartek, J. (2004) Checking out the Centrosome. *Cell Cycle*, **3**, 1390–1393.
38. Tapon, N., Ito, N., Dickson, B.J., Treisman, J.E. and Hariharan, I.K. (2001) The *Drosophila* tuberous sclerosis complex gene homologs restrict cell growth and cell proliferation. *Cell*, **105**, 345–355.
39. Wataya-Kaneda, M., Kaneda, Y., Hino, O., Adachi, H., Hirayama, Y., Seyama, K., Satou, T. and Yoshikawa, K. (2001) Cells derived from tuberous sclerosis show a prolonged S phase of the cell cycle and increased apoptosis. *Arch. Dermatol. Res.*, **293**, 460–469.
40. Dietrich, C.U., Krone, W. and Hochsattel, R. (1990) Cytogenetic studies in tuberous sclerosis. *Cancer Genet. Cytogenet.*, **45**, 161–177.
41. Debiec-Rychter, M., Jesionek-Kupnicka, D., Zakrzewski, K. and Liberski, P.P. (1999) Cytogenetic changes in two cases of subependymal giant-cell astrocytoma. *Cancer Genet. Cytogenet.*, **109**, 29–33.
42. Popper, H.H., Gamperl, R., Pongratz, M.G., Kullnig, P., Juttner-Smolle, F.M. and Pfragner, R. (1993) Chromosome typing in lymphangiioleiomyomatosis of the lung with and without tuberous sclerosis. *Eur. Respir. J.*, **6**, 753–759.
43. Dal Cin, P., Sciort, R., Van Poppel, H., Baert, L., Van Damme, B. and Van den Berghe, H. (1997) Chromosome analysis in angiomyolipoma. *Cancer Genet. Cytogenet.*, **99**, 132–134.
44. Debiec-Rychter, M., Saryusz-Wolska, H. and Salagiński, M. (1992) Cytogenetic analysis of renal angiomyolipoma. *Genes Chromosomes Cancer*, **4**, 101–103.
45. Huang, Y.S. and Richter, J.D. (2004) Regulation of local mRNA translation. *Curr. Opin. Cell Biol.*, **16**, 308–313.
46. Groisman, I., Huang, Y.S., Mendez, R., Cao, Q., Theurkauf, W. and Richter, J.D. (2000) CPEB, maskin, and cyclin B1 mRNA at the mitotic apparatus: implications for local translational control of cell division. *Cell*, **103**, 435–447.
47. Kwiatkowski, D.J., Zhang, H., Bandura, J.L., Heiberger, K.M., Glogauer, M., el-Hashemite, N. and Onda, H. (2002) A mouse model of TSC1 reveals sex-dependent lethality from liver hemangiomas, and up-regulation of p70S6 kinase activity in Tsc1 null cells. *Hum. Mol. Genet.*, **11**, 525–534.
48. Astrinidis, A., Cash, T.P., Hunter, D.S., Walker, C.L., Chernoff, J. and Henske, E.P. (2002) Tuberin, the tuberous sclerosis complex 2 tumor suppressor gene product, regulates Rho activation, cell adhesion and migration. *Oncogene*, **21**, 8470–8476.
49. Blomberg-Wirschell, M. and Doxsey, S.J. (1998) Rapid isolation of centrosomes. In Doxsey, S.J. (ed.), *Methods Enzymol*, Academic press, New York, Vol. **298**, pp. 228–238.